J. exp. Biol. (1981), 93, 283–302
With 10 figures
Printed in Great Britain

DYNAMIC TENSILE PROPERTIES OF THE PLANTARIS TENDON OF SHEEP (*OVIS ARIES*)

By ROBERT F. KER
Department of Pure and Applied Zoology, The University of Leeds, LS2 9JT, United Kingdom

(*Received* 3 *December* 1980)

SUMMARY

1. The stresses applied during fast locomotion are sufficient to stretch the tendon far into the linear region of the load-extension plot.
2. The tangent modulus in the linear region is about 1·65 GN.m^{-2} and is independent of frequency for oscillations in the range 0·22 to 11 Hz.
3. Internal damping dissipates about 7% of the mechanical energy applied during oscillations. The load range (0 to about 1 kN) and frequencies (0·22 to 11 Hz) were comparable to those arising during locomotion.
4. The rate of rise of temperature, during the initial period of an oscillation, was consistent with the mechanical measurement of power loss.
5. The dynamic mechanical properties are appropriate for the hypothesis of energy saving by storage in tendons during fast locomotion.

1. INTRODUCTION

Mammals of intermediate size save energy during running by using elastic stores (see, for example, Cavagna, Heglund & Taylor, 1977). The main energy stores are probably tendons rather than the contractile fibres of muscles (Alexander & Bennet-Clark, 1977; Morgan, Proske & Warren, 1978). The aim of this paper is to provide data on the material properties of tendons relevant to this function.

The possible candidates, as energy stores during running, are those tendons stretched during the early part of each step. I chose the plantaris tendon of the sheep. It is of suitable size for the equipment available. The plantar portion is long compared to its thickness and is reasonably uniform; at each end (the regions of the heel and the toes) there is a wider part which proved useful for clamping. The data required are for tensile stiffness and internal damping under loading conditions comparable to those in locomotion.

The plantaris tendon is subject to longitudinal oscillations. The load is presumably zero while the foot is off the ground. If the stride frequency is f and the duty factor is β, the load rises and falls to zero again in a time of β/f. To achieve the same rates of change in a sinusoidal oscillation the frequency would have to be f/β. Alexander, Jayes & Ker (1980) give data for a fast galloping dog for which f can be calculated to be 2·9 Hz and β is 0·23. The equivalent continuous frequency is 13 Hz. It is unlikely a sheep could perform so well; frequencies up to 11 Hz were used. The stress in the plantaris tendon of an antelope galloping fast is between 50 and 100 $MN.m^{-2}$. Th[e] values have been amended from those in Alexander (1977) by using 1120 $kg.m^{-3}$ for the density of moist tendon (Table 1, section 3.1) instead of 1420 $kg.m^{-3}$. Information is not available for fast moving sheep, but a comparable maximum stress seems probable. Since the plantaris tendon of sheep has a cross-sectional area of about 18 mm^2 (Table 1), a stress of 75 $MN\cdot m^{-2}$ means a load of 1·4 kN. (In practice, to avoid anxiety about the integrity of the specimen, I was content with less than 1·4 kN.)

Two previous attempts have been made to measure the internal damping in tendons, both of which gave high values. Cuming, Alexander & Jayes (1978), using the interosseous muscle of the foreleg of the sheep, found that 38% of the energy used to stretch the tendon was dissipated. The corresponding quantity from the work of Schwerdt, Constantinesco & Chambron (1980) is about 24%, using human digital tendons. For very different reasons, to be discussed in section 4.2, neither result can be taken as representative of a 'typical' leg tendon. Other information on the mechanical properties of tendons is reviewed by Wainwright *et al.* (1976). None of this relates directly to the function of tendons in locomotion, since the experiments were carried out at low rates of strain.

2. MATERIALS AND METHODS

2.1 *General*

Forced longitudinal oscillations were applied to the tendon by a servo-hydraulic tensile test machine (Fig. 1*a*). The plantar portion of the tendon was held by its two ends; the regions from near the heel and toe respectively. However, only part of this length, defined by the position of an extensometer (section 2.4), constitutes the test-piece. I used a range of test-piece lengths, up to 40 mm, keeping the mid-point approximately constant. Load measurements were made beyond the static clamp; inertial effects are negligible at the amplitudes and frequencies used. A hysteresis loop is obtained by plotting simultaneous measurements of load versus extension (Fig. 1*b*); in such a plot, slopes relate to stiffness and areas to energy. The area of the hysteresis loop represents the mechanical energy converted into heat in the test-piece.

2.2 *Tendons*

Some details concerning the sheep used and their plantaris tendons are included in Table 1 (section 3.1). The sheep lived in lowland fields for at least their first 9 months. Thereafter they were in small pens for the times stated in Table 1. The tendons were either used within 24 h of the death of the sheep, in which case they are described as 'fresh', or the legs were stored frozen until required. During dissection the tendons were kept moist using a solution of 0·9% sodium chloride in water. This solution was also applied, at a rate of 1 $ml.min^{-1}$, to the top of the tendon during mechanical testing. The saline seeped down over the whole surface.

For each tendon subjected to mechanical testing, its pair from the other hind leg of the same sheep was used for the measurement of cross-sectional area. So far as possible, the corresponding portions of both tendons were dissected out; each was weighed to establish the comparability, or otherwise, of the two tendons. The wid[ths] and thicknesses were approximately measured with vernier calipers. A more detailed

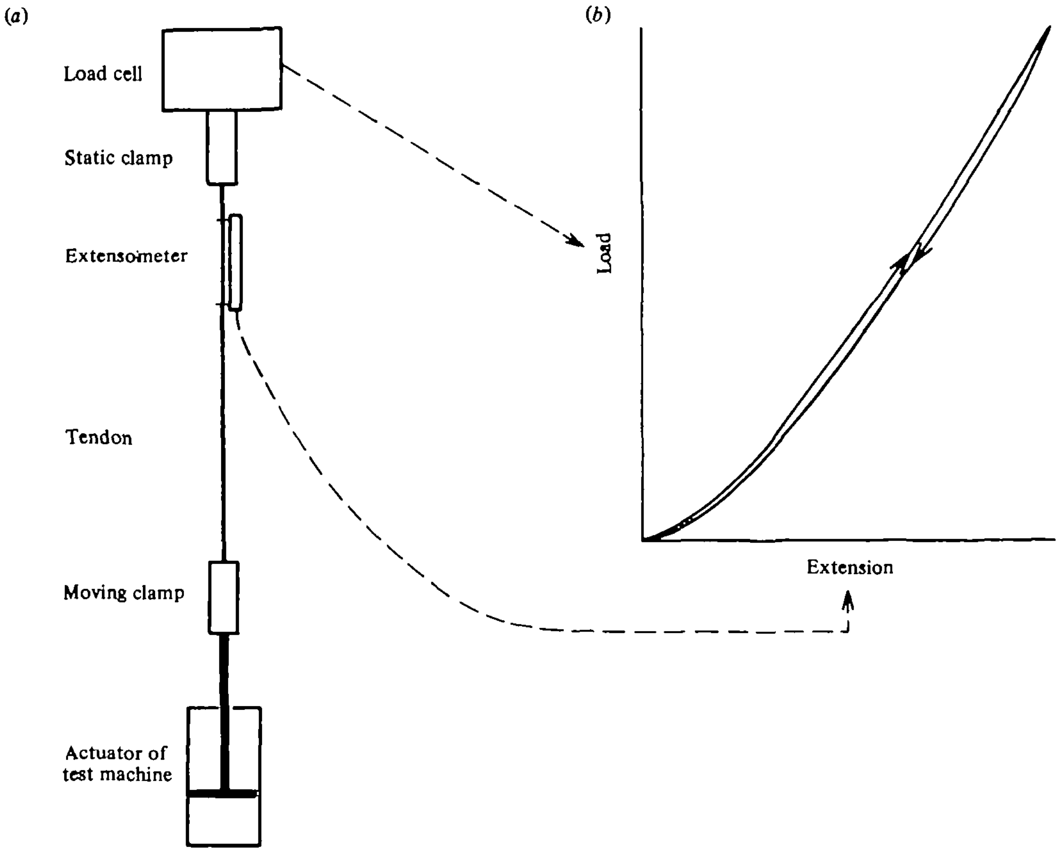

Fig. 1. Principle of the measurements. (*a*) A tendon in the servo-hydraulic tensile test machine. The upper end is clamped at the heel region: the lower at the toe region. (*b*) A hysteresis loop. The arrows show the direction of movement of the pen as the loop is drawn.

gravimetric method of finding cross-sectional area was also applied to each 'pair'. Three portions, of length 13 to 20 mm, were cut from the region corresponding to the test-piece. Each portion was weighed and its length was measured with vernier calipers. Its density, while moist, was measured by flotation in a chloroform-benzene mixture. Ellis (1969) found that the gravimetric method gives the most reliable cross-sectional area for moist tendon. The cross-sectional areas obtained gravimetrically were less than (width × thickness) as measured with the vernier calipers, usually by about 5%. In one case, marked with an asterisk in Table 1, the masses of the paired tendons were not consistent and the value given is the vernier measurement on the test-piece (reduced by 5%). Otherwise, the gravimetric measurements on the 'pair' were preferred.

2.3 *Clamps*

The design of the clamps was adapted, for the plantaris tendon, from a version used in the Bioengineering Group at Leeds University. Each clamp consists of two plates, one of steel and the other of dural, forced together by two steel bolts 32 mm apart (Fig. 2*a*, *b*). The final 5 mm to the tips of the jaws are angled slightly outwards. Part

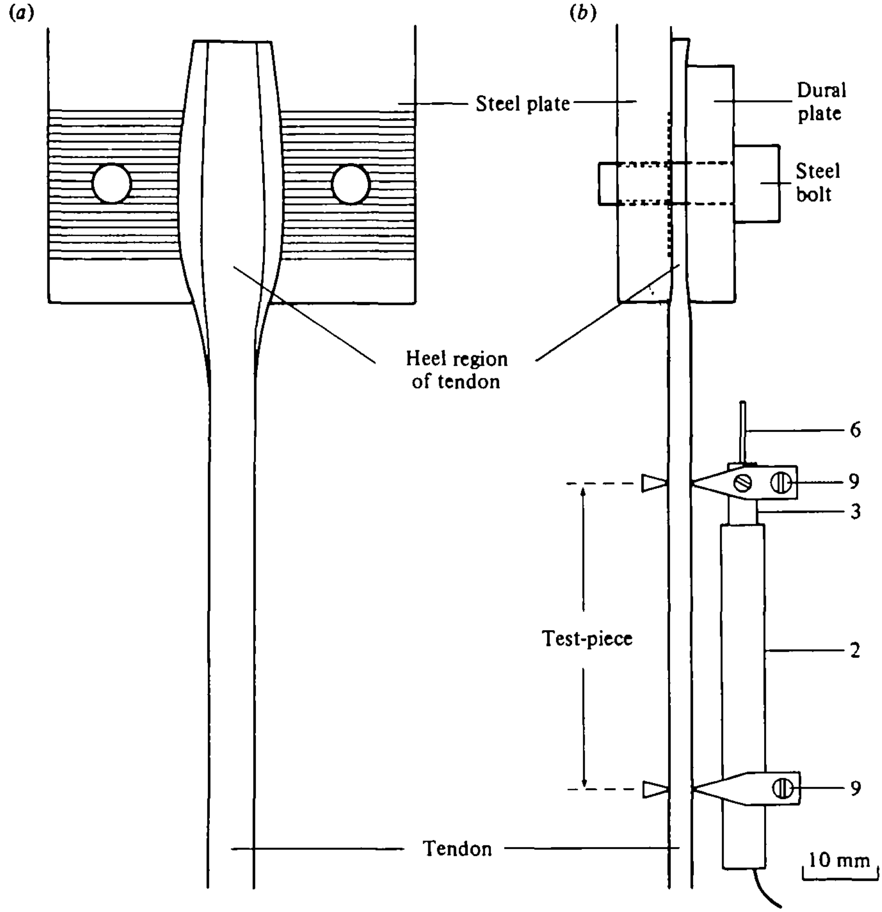

Fig. 2. (*a*) The tendon and the steel plate of the upper main clamp (front view). (*b*) The main clamp and the extensometer (side view). The striations are shown symbolically by a dashed line – as for tapped holes. The clearance between the steel and dural plates is that in the centre of the clamp: the dural plate bends slightly, reducing the gap at the sides. The numbers for the parts of the extensometer are listed in the legend to Fig. 3. The shape of the jaws of the extensometer clamps is shown for the region of contact with the tendon. Screws (10) and pins (13) (Fig. 3*b*) are omitted.

of the steel plate is serrated as shown in Fig. 2. The clamps were applied to the broader regions at each end of the plantar portion of the tendon. The increase in width, which is most marked for the end from near the toes, is an advantage for clamping. In addition, these regions, especially the end from around the heel, are more resistant to lateral compression than 'typical' tendon. The dural plate is flexible enough to become slightly bent, in partial conformity to the shape of the tendon, when the bolts are highly tightened. For this reason it was preferable to a second steel plate.

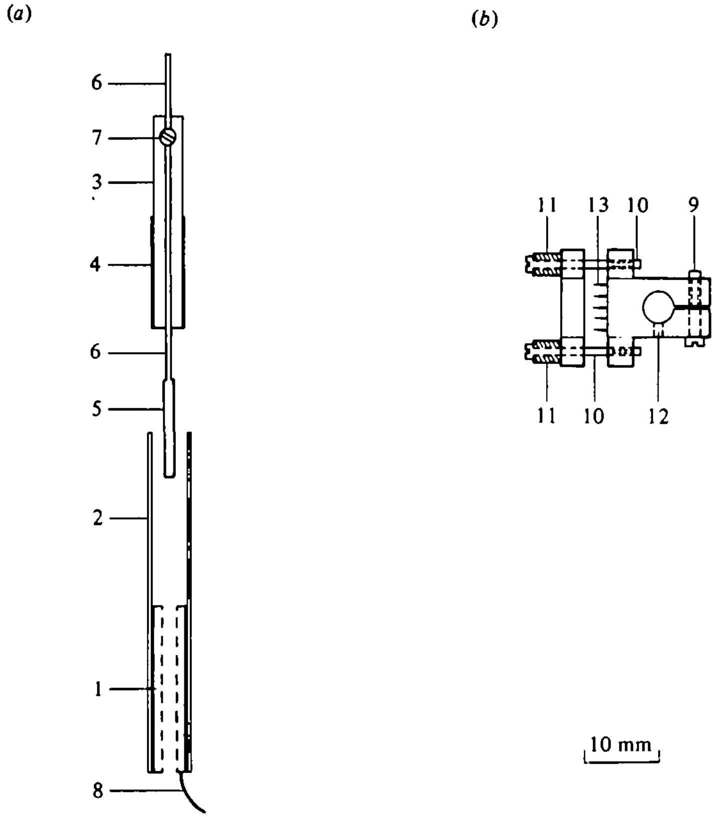

Fig. 3. The extensometer. (*a*) Side view; pulled out. Without the clamps the main parts are coaxial cylinders. The body (1) of the LVDT is held in the steel outer tube (2). The dural inner tube (3) carries a PTFE coat (4) to ensure low friction. The core (5) of the LVDT has an extension rod (6) which is held by the screw (7). In use, tube (3) moves within tube (2); the LVDT output, carried by the wires (8), varies proportionately. The zero reading is set by adjusting the position of the rod (6) within the tube (3). (*b*) The upper extensometer clamp (top view). The clamp is made of dural. Screw (9) secures the clamp to tube (3). The jaws are connected by screws (10) supported in blocks. The left-hand jaw slides on screws (10); pressure is maintained by compression of the rubber tubes (11). The hole (12) allows screw (7) to reach tube (3). Pins (13) penetrate $\frac{1}{3}$ of the thickness of the tendon. The lower extensometer clamp is identical, except that it fits to the outer tube (2) and there is no hole (12). Its position on tube (2) is adjustable.

2.4 *Extensometer*

The extensometer is shown in Figs. 2 and 3. It was built round a Schaevitz XS-B sub-miniature linear variable differential transformer (LVDT), capable of measuring displacements of $\pm 2 \cdot 5$ mm. The design criteria were: (i) low mass (6·2 *g* and 3·3 *g* for the parts with the body and the core of the LVDT respectively); (ii) mass as near to the tendon as possible; (iii) positive guidance to allow only linear movement of the core relative to the body of the LVDT; (iv) variable gauge length (10 to 40 mm); (v) unrestricted pull-out in case the specimen breaks within the gauge length. (Fig. 3*a* shows the extensometer 'pulled-out' for clarity.)

A crucial feature of the design are the clamps to attach the extensometer to the tendon (Figs. 2*b* and 3*b*). These have flat faces 0·5 mm long (Fig. 2*b*) and 8 mm wide (slightly more than the full width of the tendon). Five sharp steel pins (Fig. 3*b*, part 13) of base diameter 0·3 mm project from the face on the extensometer side and penetrate some ⅗ of the way through the tendon. As a check on the wisdom of using pins, I made measurements before and after inserting a number of extra pins through the test-piece. The results were unaltered.

The test-piece length is the distance between the centres of the extensometer clamps. This distance can be varied by fixing the lower clamp (Fig. 2*b*) at different positions on the main tube (part 2). I measured the test-piece length (with vernier calipers) when the tendon was subjected to a load of 0·1 kN – just enough to keep it taut. The LVDT was calibrated using a travelling microscope.

2.5 *Tensile test machines and electronics*

Oscillations at the higher frequencies (up to 11 Hz) were provided by a servo-hydraulic tensile test machine made by RDP-Howden Ltd. Up to 1·1 Hz, I used a large machine (Dartec Ltd) fitted with a low capacity load cell made by Transducers (C.E.L.) Ltd. After this modification both machines had a similar load capacity of about 2 kN. The load calibrations were checked against each other by using the same steel spring in each machine. The readings on the Dartec were also checked against a spring balance, with maximum load 0·87 kN, and found to be correct to within 2%.

The machines were operated under displacement control, with their actuators moving sinusoidally. In most tests the tendon was allowed to go fully slack, though not for as long as must happen when the sheep is running. This results in the time course of the extensions of the test-piece being a distorted sine wave, flattened around the minimum. In addition, clamp effects must cause slight further departures from proportionality between the actuator and test-piece movements. The load is less nearly sinusoidal because of the non-linearity of the load-extension curve for tendon. When the tendon becomes fully slack, it bends – except for the test-piece, which is restrained by the extensometer.

The signals from the load cell and the LDVT were recorded digitally by a pair of synchronoized transient recorders (DL 901 from Datalab Ltd). The data was subsequently plotted from the transient recorders on to an X–Y plotter to give a hysteresis loop as shown schematically in Fig. 1*b*.

An untoward phase shift in the measurement system could lead to grossly incorrect values for energy dissipation. To check, I used the system with a steel, helical spring in place of the tendon. Initially this gave a large loop at the higher frequencies used (6·6 and 11 Hz). However, a modification to the load cell circuit reduced the loops to an acceptable, though not negligible, size. The necessary correction is described in section 3.3. A steel spring would be expected to give no observable loop with the recording method used. The loss coefficient in torsion for steel is about 0·001 (see Lazan, 1968). This corresponds to an energy dissipation, in measurements like those to be described for tendons, of only 0·16% (section 4.2). Internal energy dissipation for metals is virtually independent of frequency over the range of my experiments (Kimball & Lovell, 1927). Dynamic effects would be expected to be small, though as small as with tendons as the spring is more massive. In any case, since accelerations are matched by decelerations, inertia cannot, on its own, produce a net hysteresis loop. Any loop in the load-extension plot observed, when using the steel spring, must be attributed to the measurement system and not to the steel.

2.6 *Temperature rise experiments*

When mechanical energy is lost, heat is produced. This gives an opportunity to assess the energy loss by a method entirely independent of that described above. It, therefore, provides a valuable check on the absence of gross systematic errors.

The tendon used for this check was first subjected to mechanical measurements at 3 load ranges and a frequency of 1·1 Hz. (It is tendon 6 in Tables 1 and 2.) The extensometer and saline drip were then removed. A fine copper-constantan thermocouple junction was inserted into the tendon. Next the tendon was wrapped in plastic film to prevent evaporation, followed by shiny aluminium foil in an attempt to reduce heat losses. Finally, a cardboard cylinder of diameter about 40 mm and closed as far as possible at both ends was fitted around the tendon to reduce air currents. The thermocouple formed part of an electric thermometer (Comark Ltd), through which the temperature of the tendon was plotted as a function of time on a chart recorder. After waiting for the temperature to become constant with the system static, oscillations were started at one of the load ranges used in the initial mechanical measurements and at a frequency of 1·1 Hz. Other power inputs were achieved by using the other load ranges and frequencies of 0·55 to 2·2 Hz. In this experiment the tendon was not allowed to go slack for fear of dislodging the thermocouple junction; though, in practice, it stayed in place well.

3. RESULTS

3.1 *Plots of load cell versus extensometer readings*

Fig. 4 is an example of the read-out from the X–Y plotter. The arrows show the direction of movement of the pen while the loop was being drawn. Load leads extension, as is necessary when mechanical energy is lost in the test material. Note the pointed ends to the loop; at the extremes, load and extension are in phase. This is not unusual. Pointed hysteresis loops are found, for example, with metals and with rubbers at high stress (Lazan, 1968). The experiments were done at room temperatures between 18 and 24 °C. One set of readings, with tendon 5, was repeated after the room temperature had been raised as much as practical – to 32 °C. For these readings the tendon was wrapped in plastic film to reduce cooling by evaporation. There was no change in the hysteresis loops.

For tendons 1 to 4 (Table 2), at each of the stated frequencies I made plots like Fig. 4 at a range of test-piece lengths. The consistency of the results to be presented in the next two sub-sections will be assessed by linear regression against test-piece length. Compliance (i.e. extension/load) is used in section 3.2, rather than stiffness, because, for a uniform tendon, linear variation with length is expected.

Repeatability was confirmed by returning after a series of measurements to the test-piece length used initially. There is no evidence for any effect such as stress softening over a period of the order of 2 h and 10^4 oscillations. I have not made

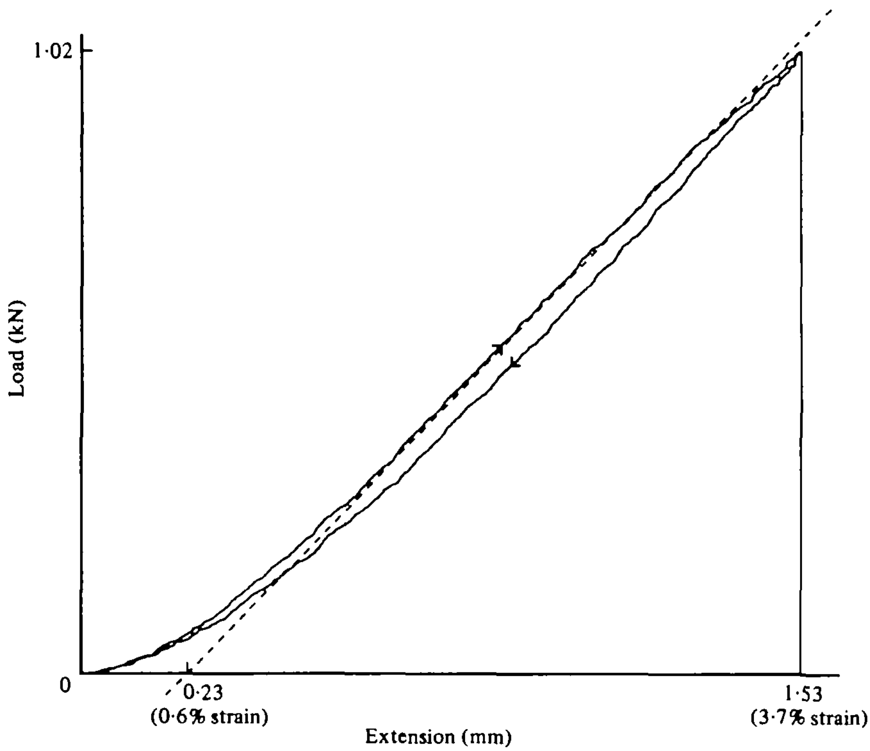

Fig. 4. A hysteresis loop. Tendon 3; frequency 1·1 Hz; test-piece length 41·0 mm. The dashed, straight line extrapolates the linear region of the loading curve. The arrows show the direction of movement of the pen as the original loop was being plotted.

Table 1. *The sheep and tendons*

	Sheep					Plantaris tendon	
Tendon number	Sex	Mass of sheep, kg	Age, years	Time in pen, months	Leg fresh or stored frozen	Density (pair), kg.m⁻³	Cross-sectional area, mm²
1	♂	50	2	12	Frozen	1140	19·4
2	♂	50	1	0·75	Fresh	1100	20·6
3	♀	40	5	0·4	Fresh	1120	16·8
4	♀	50	5	2	Fresh	1120	16·7*
5	♀	45	5	0·75	Fresh	1130	19·4
6	♀	60	5	0·1	Frozen	1130	17·0

Breeds: the sheep providing tendon 1 was (Eastfriesan × Blackface) the others were (Damline × Blackface).

* There is some doubt about this area (see text).

measurements during the first few oscillations of a test period since these inevitably take place while adjustments are being made to the settings of the test machine. Any short term effect would have little relevance to steady locomotion.

Table 2. *Mechanical data for the plantaris tendon of the sheep*

(95 % confidence limits are shown for tendons 1 to 4. The results for tendons 5 and 6 were obtained with a single test-piece length.)

Tendon number	Frequency, Hz	Minimum load, kN	Maximum load, kN	Compliance/length, c, MN^{-1}	Tangent modulus, E, $GN.m^{-2}$	Loading area/length, a_l, $J.m^{-1}$	Loop area/length, a, $J.m^{-1}$ (= N)	Energy lost/length per cycle, a_d, $J.m^{-1}$ (= N)	Percentage energy dissipation
1	1	0·07	0·65	26·5 ± 5·8	1·95 ± 0·43	6·07 ± 0·86	0·48 ± 0·14	0·48 ± 0·14	7·9 ± 2·5
	10	0·07	0·65	25·9 ± 7·8	1·99 ± 0·60	5·55 ± 0·69	0·57 ± 0·080	0·35 ± 0·080	6·3 ± 1·6
2	0·22	0	0·66	35·5 ± 2·6	1·37 ± 0·10	8·31 ± 0·67	0·46 ± 0·19	0·46 ± 0·19	5·5 ± 2·3
	1·1	0	0·66	35·3 ± 4·1	1·38 ± 0·16	7·99 ± 1·11	0·48 ± 0·19	0·48 ± 0·19	6·0 ± 2·5
3	0·22	0	1·02	30·2 ± 5·0	1·97 ± 0·33	18·9 ± 1·7	0·76 ± 0·28	0·76 ± 0·28	4·0 ± 1·5
	1·1	0	1·02	30·9 ± 5·7	1·93 ± 0·36	17·5 ± 2·2	1·01 ± 0·39	1·01 ± 0·39	5·8 ± 2·4
4	1·1	0	0·71	40·2 ± 8·3	1·49 ± 0·31	10·0 ± 1·1	0·73 ± 0·39	0·73 ± 0·39	7·3 ± 4·0
	6·6	0	0·71	41·5 ± 7·6	1·44 ± 0·26	10·9 ± 2·4	1·08 ± 0·42	0·90 ± 0·42	8·3 ± 4·3
	11	0	0·71	39·6 ± 9·8	1·51 ± 0·37	10·7 ± 2·4	1·36 ± 0·42	0·91 ± 0·42	8·5 ± 4·4
5	1·1	0	0·71	37·3	1·38	9·95	0·57	0·57	5·7
	6·6	0	0·71	37·4	1·38	10·1	0·98	0·81	8·0
	11	0	0·71	36·8	1·40	10·1	1·16	0·73	7·2
6	1·1	0·10	0·70	33·6	1·75	6·23	0·38	0·38	6·1
	1·1	0·13	0·85	34·5	1·71	8·99	0·53	0·53	5·9
	1·1	0·10	0·97	34·3	1·71	13·3	0·71	0·71	5·3

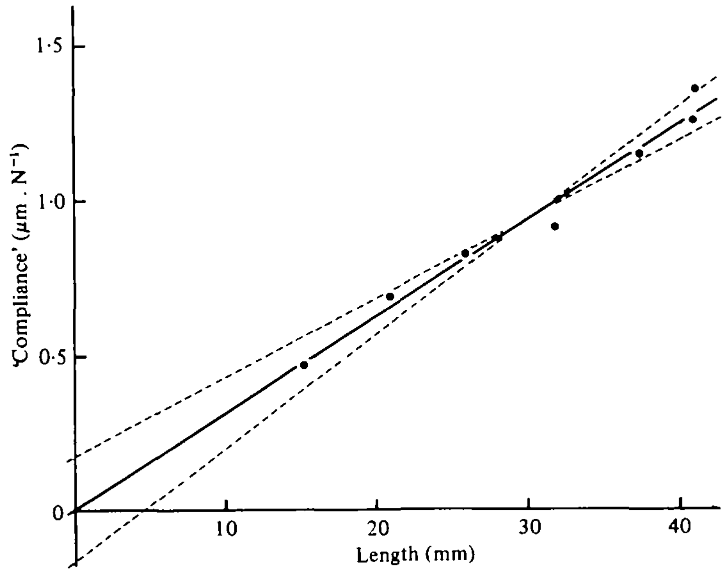

Fig. 5. 'Compliance' of the test-piece against its length. Tendon 3; frequency 1·1 Hz. The solid line is the linear regression of compliance on length. The dashed lines show the 95 % confidence limits for the slope of the regression line (with the centroid unaltered).

3.2 *Compliance*

In the hysteresis plots, the curve produced while the tendon was being stretched is nearly linear at higher loads. The dashed line in Fig. 4 extrapolates this linear region. The reciprocal of the slope of this line provides one of the points for Fig. 5. The solid line in Fig. 5 shows the linear regression of compliance on length; its slope is the compliance per unit length of the tendon (Table 2).

The dashed lines in Fig. 5 illustrate the 95 % confidence limits of the slope of the regression line, calculated by the method in Davies (1949). The values of these limits are included in Table 2. In all graphs like Fig. 5 (and those like Figs. 6 and 7 to be described below), the origin lies between the dashed lines.

In this treatment of errors no weight has been given to the origin. Clearly, the compliance of a zero length of tendon must be zero. However, there are, no doubt, systematic as well as statistical reasons why measurements may give, by extrapolation, a non-zero (positive or negative) compliance at zero length. It would be incorrect to force the regression line to go through the origin. On the other hand, I may, by giving no significance to the origin, have over-estimated the uncertainty of the results. (An alternative method of calculation would be to average compliance per unit length values obtained, individually from each reading, by dividing the compliance of the test-piece by its length. This would result in very much narrower confidence limits than those given in Table 2, because the method gives great weight to the origin. Each value is, in effect, the slope of the line joining the origin to the point in question.) To summarize, formal statistical methods are not entirely appropriate in handling these results, because of the influence of systematic as well as random effects; however, the 95 % confidence limits stated, considered in relation to the methods used should give some idea of reliability.

The tangent modulus, E in Table 2, defined as the slope of a graph of stress against strain, is $1/cS$, where c is the compliance per unit length and S is the cross-sectional area (Table 1). The confidence limits given for E are directly proportional to those for c; no allowance has been made for the uncertainty in S. The values of E apply at loads approaching the stated maxima. However, the slope does not significantly change from about 0·3 kN upwards (stress about 17 $MN.m^{-2}$). The linearity extends at least to 1·5 kN, in the case of a tendon of cross-sectional area 16·8 mm^2. This represents the highest stress (89 $MN.m^{-2}$) I have achieved while recording a rapidly formed load-extension plot. The corresponding strain was 5·3%. The ultimate tensile stress was not reached.

The results in Table 2 show the tangent modulus to be independent of frequency over the range 0·22 to 11 Hz, which covers the whole of locomotion.

The mean value of the tangent modulus (in the linear region) is 1·65 $GN.m^{-2}$. However, there is considerable variation from tendon to tendon.

3.3 *Energies*

Data contained in the hysteresis plots, such as Fig. 4, will be used in this subsection to assess (i) the energy required to stretch the tendon and (ii) the energy dissipated in each cycle. These energies are compared in (iii).

(i) For each hysteresis plot, I measured the area between the loading curve and a horizontal line at the minimum load. This will be termed the 'loading area', A_l. For tendons 2 to 5, for which the minimum load is zero, A_l is an estimate of the energy required to stretch the tendon through the full range. For tendons 1 and 6, A_l is less than the energy required to stretch the tendon from the minimum to the maximum load. However, the loading area remains the most useful energy with which to compare the energy dissipated, as will be explained in section 4.2.

In Fig. 6 loading area is plotted against test-piece length for tendon 3. The points were corrected for small variations in the maximum load, as measured on the hysteresis plots, on the assumption that area is proportional to $(\text{load})^2$. This is clearly not strictly correct, but is likely to be adequate since the variations are small. Henceforth, the treatment was parallel to that for compliance, leading to loading area per unit length of tendon (Table 2, denoted by a_l). For tendons 2 to 5, a_l is the energy required to stretch unit length of tendon through the stated load range.

(ii) Measurement of the area of the hysteresis loops led, via plots like Fig. 7, to loop area per unit length of tendon (Table 2, denoted by a). However, a correction is required, at the higher frequencies, before a can be considered as an energy.

Fig. 8 shows the loop formed using the steel spring at 11 Hz (section 2.5). Since the loop is generated within the instrumentation, either load or extension could lead. In fact, load leads as with the tendon experiments. The area of the loop generated, in tendon experiments, within the instrumentation is found by scaling the loop of Fig. 8 according to the relative loading areas obtained with the tendon and the spring. The ratio of the area of the loop to the loading area in Fig. 8 is 0·042. The correction is made by subtraction, as will be justified in section 4.2. Let a_d be the loop area per unit length due to energy dissipation within the tendon. At 11 Hz,

$$a_d = a - 0{\cdot}042\,a_l. \quad (1)$$

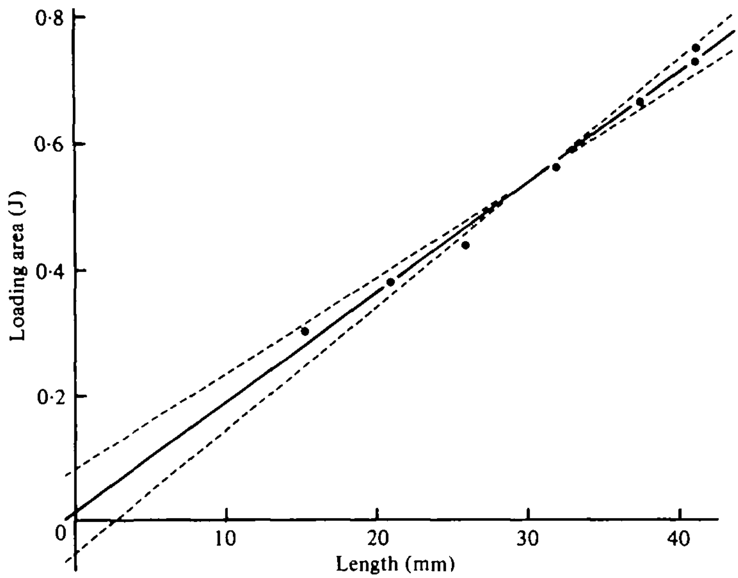

Fig. 6. Loading area of the test-piece against its length. Tendon 3; frequency 1·1 Hz. The solid line is the linear regression of loading area on length. The dashed lines show the 95% confidence limits for the slope of the regression line (with the centroid unaltered).

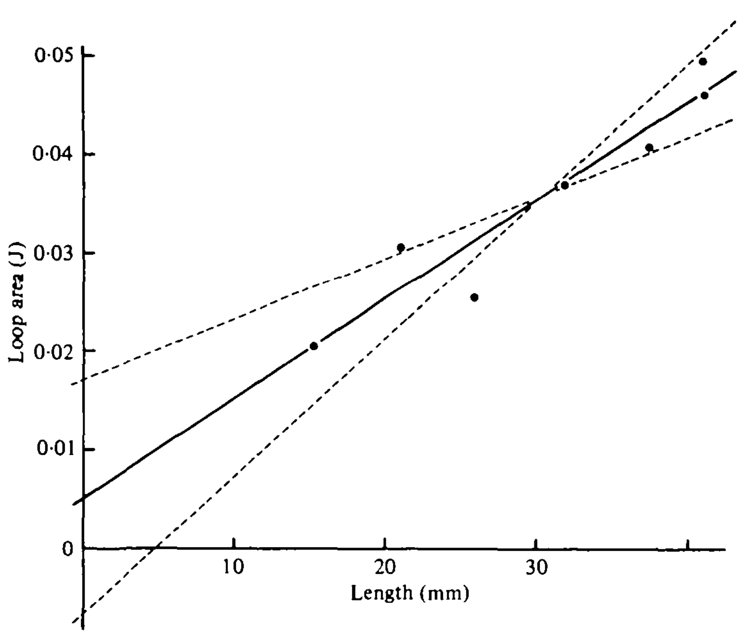

Fig. 7. Loop area of the test-piece against its length. Tendon 3; frequency 1·1 Hz. The solid line is the linear regression of loop area on length. The dashed lines show the 95% confidence limits for the slope of the regression line (with the centroid unaltered).

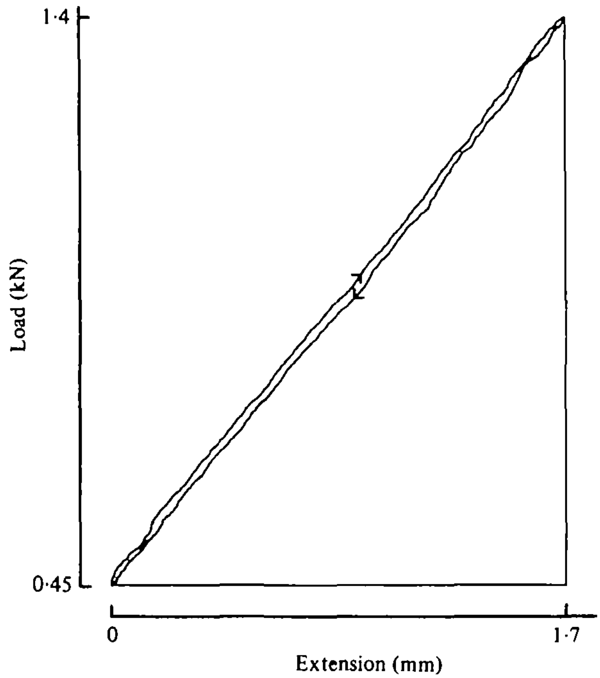

Fig. 8. Test with the steel spring at 11 Hz. The loop was generated within the instrumentation. *The zero of extension is arbitrary. The loading area is the 'triangle' delineated by the loading* curve and the lines drawn in at minimum load and maximum extension.

At 6·6 Hz the ratio 0·042 in equation 1 is replaced by 0·017 and at lower frequencies the correction is negligible. The 95% confidence limits stated in Table 2 for a_d are the same as those for a, even though the reliability of the results at 6·6 Hz and 11 Hz is clearly reduced by the need to make corrections.

(iii) The final column of Table 2 gives values of $100\,(a_d/a_l)$. For tendons 2 to 5, this is the energy dissipated expressed as a percentage of the energy required to stretch the tendon. For the other two tendons the comparison is with a slightly different energy, as explained above.

The most important feature of the results is that, from a functional point of view, the loss of mechanical energy is always small. The mean value is about 7%. With an energy loss of this magnitude tendons certainly have potential as energy stores. Within the accuracy of the measurements, the percentage energy loss is independent of frequency. However, the range within the 95% confidence limits is sufficient to allow variations from a minimum of about 4% to a maximum of about 10%. In this context, a factor of even 2·5 times is 'small' – small to measure and too small to influence the relative effectiveness of the tendon as an energy store at different running speeds.

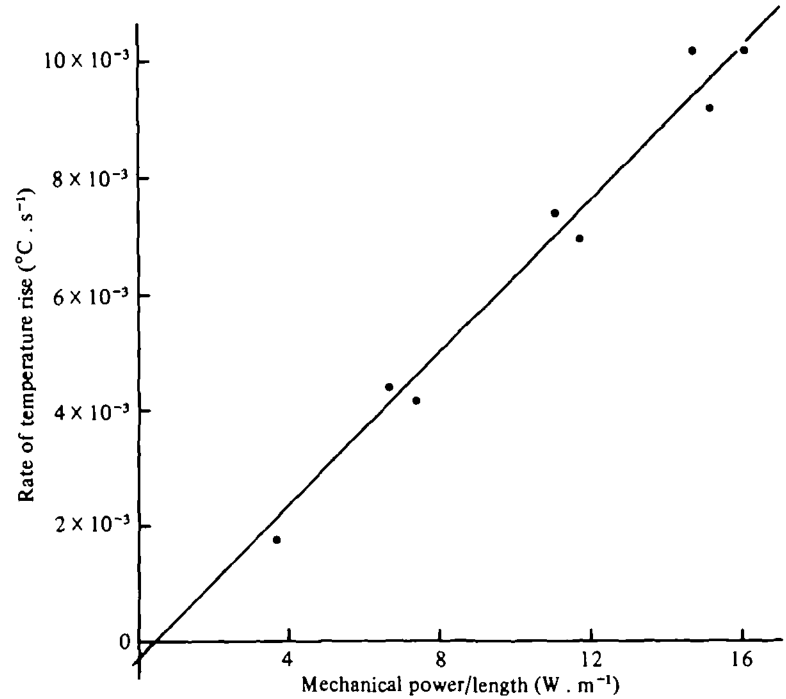

Fig. 9. Rate of temperature rise against the measurement of mechanical power applied to unit length of tendon.

3.4 *Temperature rise measurements*

At the beginning of a period of oscillation, while the excess temperature was small, the temperature-time plots appeared satisfactorily linear and were clearly related to energy input: for example, if the frequency of the oscillation was altered in mid-run, the temperature-time plot showed an abrupt and immediate change of slope.

The mechanical measurements of energy loss were compared, in section 3.3, with loading area per unit length, a_l. Here, since the *rate* of temperature rise was measured, the comparison is with the mean 'loading power' per unit length, which equals $a_l f$, where f is the frequency of the test. The values of a_l are given in Table 2 (tendon 6) for the three load ranges used. a_l is independent of frequency (Table 2, tendons 1 to 5) and, therefore, the same values apply for all the frequencies used in the temperature measurements – 0·55, 1·1, 1·65 and 2·2 Hz. In Fig. 9 the observed rate of rise of temperature is plotted against $a_l f$. The slope of the linear regression of rate of temperature rise on loading power is $(6{\cdot}60 \pm 0{\cdot}79) \times 10^{-4}$ °C. N^{-1} ($\pm 95\%$ confidence limits). (Linearity depends on the energy dissipation per cycle being independent of frequency and of load range). In calculating the regression line, the origin was given the same weight as the experimentally measured points – the rate of temperature rise is zero when the power input is zero.

To complete the comparison, the slope of the regression line must be multiplied by the heat capacity per unit length. The mass per unit length, measured as usual on the pair to tendon 6, was 0·019 kg.m^{-1}. Using the method of mixtures, I measured specific heat of the plantaris tendons of another sheep as $3{\cdot}1 \times 10^3$ J.°C^{-1}.kg^{-1}. From these values, the power dissipation is 3·9% of the loading power. This figure is to be compared with the percentage energy dissipations given in Table 2.

A lower value from the temperature measurements is to be expected for the difficulty is to observe the full temperature rise. The result is satisfactory; it gives confidence in the basic validity of the mechanical measurements.

4. DISCUSSION

4.1 *Tangent modulus*

For the plantaris tendon the average tangent modulus in Table 2 is 1·65 GN.m^{-2}. The spread in values for individual plantaris tendons is of the order of ±20%.

Rigby *et al.* (1959) found the tangent modulus of rat tail tendon to be 0·8 ± 0·2 GN.m^{-2} in the linear region at a straining rate of 10% per min. With rat tail tendon the length of specimens can be very much greater than their thickness, which reduces the need for an extensometer in mechanical tests. However, as a check, measurements over a range of lengths with a single specimen would be desirable.

With relatively thicker tendons, extensometers become more necessary. They have been used, with digital flexor and extensor tendons from humans and cats, by VanBrocklin & Ellis (1965), Matthews & Ellis (1968) and Benedict, Walker & Harris (1968). Tangent moduli of the order of 1 GN.m^{-2} were obtained. The results, however, are not directly comparable to those reported here, because the measurements were all made when the rate of loading was far less than is relevant in locomotion. Use of an extensometer circumvents many, but not all, of the potential errors associated with the interaction of the tendon and the clamps. Suppose the clamp effectively grips only half the tendon. Then, if the transfer of stress laterally across the tendon is negligible, half the full stiffness value will be recorded. Whether this problem arises depends on the properties of the tendon and the design of the clamps. In this respect, use of the toe and heel regions of the plantaris of the sheep for clamping is advantageous.

VanBrocklin & Ellis (1965) observed an increase in the tangent modulus with loading rate. In contrast, I observed no change in the tangent modulus, in the linear region, with frequency of oscillation. However, my minimum loading rate was 9 times faster than the maximum used by VanBrocklin & Ellis.

The detailed shape of the load-extension curve varies for different tendons. For example, striking changes occur with age in rat tail tendons (Torp *et al.* 1975). However, a 'toe region' is always found, in which the compliance is highest for very low loads. Diament *et al.* (1972) showed this to be due to crimping of the collagen fibres. The load-extension plots for the plantaris tendon (for example, Fig. 4) have a clear toe region, but it does not make a major contribution to the energy storage capacity of the tendon. The area between the loading curve and the extrapolation of the linear region may be considered as the contribution made by the toe region to the energy storage. In Fig. 4, this area is 0·027 J whereas the total loading area is 0·73 J. The maximum load reached during locomotion, is likely to be higher than in Fig. 4, in which case the importance of the contribution of the toe region to the energy storage will be less. The energy storage capacity of the tendon is not primarily due to straightening out the crimp, but to the elastic properties of the straightened collagen fibres. (Note this does not rule out other functions for the toe region in locomotion.) The effect of straightening out the crimp can also be assessed in terms of strain. The extrapolated linear region intercepts the extension axis at 0·6 %; the maximum strain reached in Fig. 4 is 3·7 %.

Compared to other biological structural materials used in tension, tendon is rather compliant (see Wainwright *et al.* 1976, for a survey). Wood, bone and arthropod cuticle are all of the order of ten times stiffer. Functionally, compliance in the material can be compensated by making the part thicker.

4.2 *Energy dissipation*

So far, problems of nomenclature have been avoided by treating the plantaris tendon on its merits. The methods are directly related to the function of the tendon: the quantities listed in Table 2 come directly from the measurements. However, to compare tendons with other materials the nomenclature for measures of internal damping must first be reviewed.

The measure most closely related to percentage energy dissipation is 'rebound resilience' (Alexander, 1968). From its definition, rebound resilience is simply (100 − percentage energy dissipation). The relationship to other measures is rarely straightforward and is sometimes not strictly definable (Lazan, 1968).

The nomenclature will be illustrated for a material to which sinusoidal load and extension oscillations can simultaneously be applied. (This cannot be done with tendon with its non-linear load-extension curve.) For such a material, the hysteresis loop is an ellipse. Fig. 10 shows an ellipse centred on the origin. The percentage energy dissipation represented by the ellipse will now be calculated according to the definition used for tendons. A line has been drawn joining the points on the ellipse, where the extension reaches its extreme values. Let A_t be the area of the right-angled triangle, outlined in Fig. 10, for which this line is the hypotenuse. Let A_e be the area of the ellipse. For the ellipse:

$$\text{Percentage energy dissipation} = \frac{A_e}{A_l} \times 100 = \frac{A_e}{A_t + \frac{1}{2}A_e} \times 100. \qquad (2)$$

(Note. Loading area is here considered in terms of the extremes of ***extension***. For tendon, extremes of extension and load occur simultaneously, so the distinction does not arise.)

For the ellipse of Fig. 10, A_e/A_t is 0·33 and therefore, using equation 2, the energy dissipation is 28 %.

For a linear material, A_t and A_e are independent of the position of the origin. If the origin is moved to the point on the ellipse where the extension is at its minimum, equation 2 is unchanged but A_t can now be interpreted as the energy required to stretch the tendon through the full range from zero. This is why loading area was used in considering the results from tendons 1 and 6, where the minimum load was not zero. If tendon was a linear material, the measures of internal damping for tendons 1 and 6 would be the same as for the other tendons.

All the measures of internal damping discussed by Lazan (1968) are definable for a material with an elliptical hysteresis loop. In the following list, measures identical

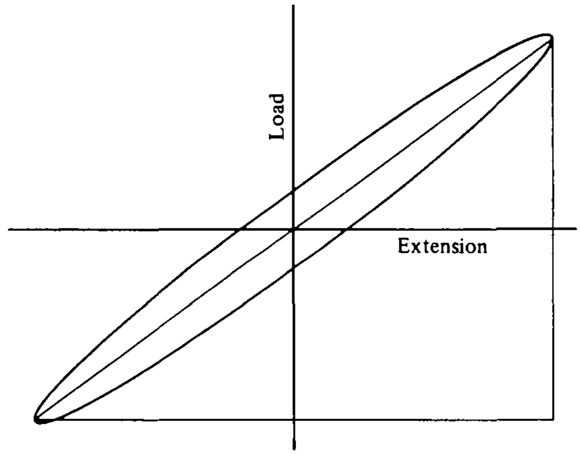

Fig. 10. An elliptical hysteresis loop.

for such a material are grouped together. They are not necessarily synonymous (even if definable) for other materials. Lazan (1968) defines all these terms (and many more) and derives the stated formulae, applicable with an ellipse.

$$\text{Relative damping} = A_e/A_t \times 100. \quad (3)$$

$$\left.\begin{array}{l}\text{Loss coefficient}\\ \text{Loss tangent}\\ \text{Ratio of loss to}\\ \text{storage moduli}\end{array}\right\} = 2A_e/\pi A_t. \quad (4)$$

$$\text{Logarithmic decrement} = 2A_e/A_t. \quad (5)$$

$$\left.\begin{array}{l}\text{Phase angle}\\ \text{Loss angle}\end{array}\right\} = \tan^{-1}(2A_e/\pi A_t). \quad (6)$$

Equation 6 will first be used to assess the acceptability of the correction applied to the measured loop areas at the higher frequencies (equation 1; section 3.3). The phase shift, ϕ, which gives rise to the observed loop, is the sum of the phase shift, ϕ_1, due to the material (here supposed linear) and ϕ_2 due to the load measuring system. Thus, $\phi = (\phi_1+\phi_2)$ and therefore,

$$\tan\phi = \frac{\tan\phi_1+\tan\phi_2}{1-\tan\phi_1.\tan\phi_2}. \quad (7)$$

$\tan\phi_1$ is about 0·05; $\tan\phi_2$ is about 0·03 (from data in section 4·3 and equation 6). Thus $\tan\phi_1.\tan\phi_2 \ll 1$ and,

$$\tan\phi_1 = \tan\phi - \tan\phi_2. \quad (8)$$

From equation 6, loop areas are proportional to the tangents of the phase angles: A_t is constant since the phase shifts ϕ_1 and ϕ_2 are applied to a single load-extension curve. Equation 1 thus follows from equation 8. (A further complication arises from the non-linearity of the load extension curve for tendon. Load variations with time were not a pure sine wave with the tendon, though they were with the steel spring.

The data required for a full examination of this point are not available; it is probable the correction has been slightly underestimated.)

The plantaris tendons have energy dissipation of about 7%. For a linear material with 7% energy dissipation, equations 2 to 6 give: relative damping 7·3%, loss coefficient 0·046, logarithmic decrement 0·15 and phase angle 2·6°.

Lazan (1968) includes a compilation of data on internal damping. Sample loss coefficients are: steel 0·001; wood 0·016; nylon 0·05. Sample ratios of loss to storage moduli are: glass-resin composite 0·01; cotton 0·06; polypropylene 0·09; rubber 0·2. The internal damping of tendon is of the same order of magnitude as that of wood and cotton; though perhaps the comparison should really be made with dried tendons. In general, internal damping peaks in certain frequency ranges; however, several decades of frequency may be needed to show a particular peak (Lazan, 1968). Kimball & Lovell (1927) found very little variation with wood and celluloid (as well as metals) over a frequency range comparable to that used here. Restricted variation, within the limits given in section 3.3 and Table 2, is not unusual.

Cuming *et al.* (1978) observed the decay of natural vibrations to measure the energy dissipation in the interosseous muscle of the foreleg of a sheep. They took advantage of the natural attachments of tendon into bone at both ends to circumvent the clamping problem. They found the energy dissipation to be 38%. I do not consider this value to be characteristic of collagenous tendon. The main complication is that the interosseous muscle includes short muscle fibres as well as collagenous tendon. These muscle fibres may behave differently in life than after death. The system of Cuming *et al.* also involved bones, junctions between tendons and bones, and joints. The joints must have been loaded somewhat unnaturally after the dissections involved in preparing the specimen. The measurements of the present paper are for tendon alone, considered as an isolated material. The whole system involved in an animal must suffer greater energy dissipation, even if the muscles are considered separately. The tendon to bone attachments may be particularly important.

Schwerdt *et al.* (1980) have carried out energy dissipation measurements on human digital flexor tendons. They applied small oscillations (amplitude 0·25%) about a much larger mean strain (up to 5%). The maximum frequency was 9·5 Hz. They measured extensions, and therefore energy losses, over a region that included the clamps: they did not systematically use a range of test-piece lengths. The energy dissipation results are expressed in terms of phase angles, which they find to be typically around 12° with a minimum value of 10°. For a material with an elliptical hysteresis loop, a phase angle of 10° corresponds to an energy dissipation of 24% (equations 6 and 2). To provide a clear comparison, I carried out an experiment with a small oscillation under conditions closely similar to those of Schwerdt *et al.*, but using my extensometer and a plantaris tendon. I obtained a particularly small loop with energy dissipation, measured by the usual ratio of areas, of only 3·6%. The corresponding phase angle with an ellipitical hysteresis loop is 1·3°. Could the human digital flexor and the sheep plantaris tendon be so very different? I find this implausible. The method of Schwerdt *et al.* requires much more detailed verification than is described in their paper.

4.3 *Function of the leg tendons in locomotion*

Alexander *et al.* (1980) discuss the conditions under which tendons can act as energy stores and thus save metabolic energy during fast locomotion of a quadruped. They include a calculation for antelope, in which the energy available to be saved is compared with the energy storage capacity of the tendons. The agreement is excellent; however, both aspects of the calculation are subject to uncertainties. The energy storage capacity of the tendons, when stretched by the observed amount, is taken from Alexander (1977). If data, from the present work, on tendon density, tangent modulus and the extent of the toe region are used instead of the values assumed by Alexander, the estimate of the energy storage capacity of the leg tendons is reduced by about 35%. Agreement could perhaps be re-established by allowing for energy storage in the interosseous muscle and the toe flexors. However, in the absence of much more reliable data on a single species, the conclusion could not be strengthened. It remains that the energy storage capacity is of the correct order of magnitude. There are no data, at present, on the extension of the relevant leg tendons in fast moving sheep.

The low internal damping established in the present work is entirely appropriate to the role of tendons as energy stores. Of course, other costs are involved. There will be some energy dissipation at the tendon-bone junctions. More important, energy is used to maintain the required muscular tensions, even if the length of the muscles remains constant.

What temperature is likely to be reached within the leg tendons of a galloping sheep? The possibility of damage by over-heating was raised by Harkness (1979). The present data give an opportunity to examine this question more closely.

During the temperature rise experiments, I allowed one oscillation with a high power input to continue until the equilibrium temperature had, more or less, been reached. The final excess temperature was 3·5 °C; the average loading power per unit length of tendon was 15·1 $W.m^{-1}$ with a load range of 0·12 to 0·75 kN and a frequency of 2.2 Hz. However, the experimental conditions were deliberately chosen to minimize heat loss. This is not the case in the sheep. For an order of magnitude calculation, the skin may be considered as an infinite heat sink: it is well supplied with blood vessels. On average, the material of the tendon is perhaps 3 mm from the skin which lies against one side. The area per unit length of this side is about 6×10^{-3} m^2. If 7% of the energy is converted to heat in the tendon, (15·1 × 0·07) W have to be removed by thermal conduction, Suppose the thermal conductivity of the tissue is that of water, 0·6 $W.m^{-1}.°C^{-1}$. Then:

$$\text{Excess temperature} = \frac{15{\cdot}1 \times 0{\cdot}07 \times 3 \times 10^{-3}}{6 + 10^{-3} \times 0{\cdot}6} = 0{\cdot}9\ °\text{C}.$$

The maximum stride frequency of a sheep is probably about 2·2 Hz (see section 1). The maximum load range applied to the tendon may be twice as great as that in my experiment, in which case the final excess temperature would be increased about four times to 3·6 °C. However, using the value of energy dissipation (38%) from Cuming *al.* (1978) would lead to an estimated temperature rise of 20 °C, which might well cause damage. These results are in general agreement with the prediction of Harkness (1979).

Over-heating of tendons is most unlikely under natural conditions. If there was any risk, a more pervasive cooling system would have evolved. Muscles produce far more heat than the tendons to which they are attached; they incorporate a thorough cooling system.

Professor R. McN. Alexander initiated this work and has been a constant source of help. I have had useful discussions with Mr A. S. Jayes. A letter from Professor R. D. Harkness, anticipating some of Harkness (1979), was of value in designing the temperature rise experiments. I thank the Department of Animal Nutrition and Physiology at the University of Leeds for the supply of sheep. For access to the tensile test machines, I am grateful to Mr R. M. Seddon, Unitex Ltd, Knaresborough, and the Department of Mechanical Engineering at Leeds University. The work was carried out under a grant from the Science Research Council to Professor Alexander.

REFERENCES

Alexander, R. McN. (1968). *Animal mechanics*. London: Sidgwick & Jackson.

Alexander, R. McN. (1977). Allometry of the limbs of antelopes (Bovidae). *J. Zool., Lond.* **183**, 125–146.

Alexander, R. McN. & Bennet-Clark, H. C. (1977). Storage of elastic strain energy in muscle and other tissues. *Nature, Lond.* **265**, 114–117.

Alexander, R. McN., Jayes, A. S. & Ker, R. F. (1980). Estimates of energy cost for quadrupedal running gaits. *J. Zool., Lond.* **190**, 155–192.

Benedict, J. V., Walker, L. B. & Harris, E. H. (1968). Stress-strain characteristics and tensile strength of unembalmed human tendon. *J. Biomechan.* **1**, 53–63.

Cavagna, G. A., Heglund, N. C. & Taylor, C. R. (1977). Mechanical work in terrestrial locomotion: two basic mechanisms for minimizing energy expenditure. *Am. J. Physiol.* **233**, R243–R261.

Cuming, W. G., Alexander, R. McN. & Jayes, A. S. (1978). Rebound resilience of tendons in the feet of sheep (*Ovis aries*). *J. exp. Biol.* **74**, 75–81.

Davies, O. L. (ed.). (1949). *Statistical methods in research and production*, 2nd ed. London: Oliver & Boyd.

Diament, J., Keller, A., Baer, E., Litt, M. & Arridge, R. G. C. (1972). Collagen: ultrastructure and its relation to mechanical properties as a function of ageing. *Proc. R. Soc.* B **180**, 239–315.

Ellis, D. G. (1969). Cross-sectional area measurements for tendon specimens: a comparison of several methods. *J. Biomechan.* **2**, 175–186.

Harkness, R. D. (1979). Mechanical properties of connective tissue in relation to function. In *Fibrous proteins: scientific, industrial and medical aspects* (ed. D. A. D. Parry and L. K. Creamer), Vol. 1, pp. 207–230. London: Academic Press.

Kimball, A. L. & Lovell, D. E. (1927). Internal friction in solids. *Phys. Rev.* **30**, 948–959.

Lazan, B. J. (1968). *Damping of materials and members in structural mechanics*. Oxford: Pergamon Press.

Matthews, L. S. & Ellis, D. (1968). Viscoelastic properties of cat tendon: effects of time after death and preservation by freezing. *J. Biomechan.* **1**, 65–71.

Morgan, D. L., Proske, U. & Warren, D. (1978). Measurements of muscle stiffness and the mechanism of elastic storage of energy in hopping kangaroos. *J. Physiol., Lond.* **282**, 253–261.

Rigby, B. J., Hirai, N., Spikes, J. D. & Eyring, H. (1959). The mechanical properties of rat tail tendon. *J. gen. Physiol.* **43**, 265–283.

Schwerdt, H., Constantinesco, A. & Chambron, J. (1980). Dynamic viscoelastic behaviour of the human tendon *in vitro*. *J. Biomechan.* **13**, 913–922.

Torp, S., Arridge, R. G. C., Armeniades, C. D. & Baer, E. (1975). Structure-property relationships in tendon as a function of age. *Colston Pap.* **26**, 197–221.

VanBrocklin, J. D. & Ellis, D. G. (1965). A study of the mechanical behaviour of toe extensor tendons under applied stress. *Archs. phys. Med.* **46**, 369–373.

Wainwright, S. A., Biggs, W. D., Currey, J. D. & Gosline, J. M. (1976). *Mechanical design in organisms*. London: Arnold.